Published in final edited form as:

Oncogene. 2013 January 3; 32(1): 97–105. doi:10.1038/onc.2012.24.

CXCL13 Activation of c-Myc Induce RANK Ligand Expression in Stromal/Preosteoblast Cells in the Oral Squamous Cell Carcinoma Tumor-Bone Microenvironment

Yuvaraj Sambandam[1], **Kumaran Sundaram**[1], **Angen Liu**[2], **Keith L. Kirkwood**[3], **William L. Ries**[3], and **Sakamuri V. Reddy**[1,*]

[1]Charles P. Darby Children's Research Institute, Medical University of South Carolina, Charleston, SC, USA

[2]Hollings Cancer Center, Medical University of South Carolina, Charleston, SC, USA

[3]School of Dental Medicine, Medical University of South Carolina, Charleston, SC, USA

Abstract

CXC chemokine ligand-13 (CXCL13) has been implicated in oral squamous cell carcinoma (OSCC) tumor progression and osteolysis. Tumor necrosis factor family member, RANKL (receptor activator of NF-κB ligand), a critical bone resorbing osteoclastogenic factor plays an important role in cancer invasion of bone/osteolysis. Here, we show high level expression of CXCL13 in primary human OSCC tumor specimens; however human bone marrow derived stromal (SAKA-T) and murine preosteoblast (MC3T3-E1) cells produce at very low level. Recombinant CXCL13 (0–15 ng/ml) dose dependently induced CXCR5 expression in SAKA-T and MC3T3-E1 cells. Conditioned media obtained from OSCC cell lines increased the RANKL expression and an antibody against the CXCL13 specific receptor, CXCR5 markedly decreased RANKL expression in these cells. Furthermore, CXCL13 increased hRANKL-Luc promoter activity. Superarray screening identified c-Myc and NFATc3 transcription factors upregulated in CXCL13 stimulated SAKA-T cells. Immunohistochemical analysis of OSCC tumors developed in athymic mice demonstrated RANKL and NFATc3 expression in tumor and osteoblast cells, however p-c-Myc expression specific to osteoblastic cells at the tumor-bone interface. We further identified NFATc3 expression but not c-Myc activation in primary human OSCC tumor specimens compared to adjacent normal tissue. Also, CXCL13 significantly increased p-ERK1/2 in SAKA-T and MC3T3-E1 cells. siRNA suppression of c-Myc expression markedly decreased CXCL13 induced RANKL and NFATc3 expression in preosteoblast cells. Chromatin-immuno precipitation (ChIP) assay confirmed p-c-Myc binding to the hRANKL promoter region. In summary, c-Myc activation through CXCL13-CXCR5 signaling axis stimulates RANKL expression in stromal/preosteoblast cells. Thus, our results implicate CXCL13 as a potential therapeutic target to prevent OSCC invasion of bone/osteolysis.

*Address for correspondence: Sakamuri V. Reddy, Ph.D, Charles P. Darby Children's Research Institute, 173 Ashley Avenue, Charleston, SC 29425. Ph: 843-792-8373; Fax: 843-792-7927; reddysv@musc.edu.

Conflict of Interest

The authors declare no conflict of interest with this work.

Keywords

oral squamous cell carcinoma; CXCL13; RANK ligand; c-Myc; osteoblast

Introduction

Head and neck squamous cell carcinoma (HNSCC) occurs approximately 3% of all malignancies in the US (1). Oral squamous cell carcinoma (OSCC), which contributes to 40% of all HNSCC, is associated with mucosal surfaces of the oral cavity and oropharynx (2). The etiology of OSCC involves multiple genetic alterations and an exposure to environmental carcinogens such as tobacco, alcohol, chronic inflammation and viral infections (3). OSCC tumor cells have been shown to invade maxillary and mandibular bone in a murine model (4). Nuclear factor kappaB (NF-κB) expression is upregulated in OSCC gradually from premalignant lesions to invasive cancer (5). Hepatocyte growth factor through upregulation of matrix metalloproteinases such as MMP-1 and MMP-9 promotes OSCC tumor invasion (6). Thus, malignant OSCC tumors potently invade local bone; however the molecular mechanisms of tumor-associated osteolysis of bone are unclear.

The tumor necrosis factor (TNF) family member, receptor activator of NF-κB ligand (RANKL) which is expressed on marrow stromal/preosteoblast cells in response to several osteotropic factors, is critical for osteoclast precursor differentiation to form multinucleated osteoclasts which resorb bone (7). Osteoclast activation plays an important role in several malignancies including oral cancer invasion of bone and metastasis (8). Also, MMP-7 produced by osteoclasts at the prostate tumor-bone interface has been shown to promote osteolysis through solubilization of RANKL (9). Furthermore, altered RANKL and osteoprotegerin (OPG) expression in OSCC cells facilitate osteoclastogenesis at the tumor-bone microenvironment (10). Thus, RANKL expression in the tumor-bone microenvironment plays an important role in cancer invasion of bone.

Chemokines are a superfamily of small cytokine-like proteins that interact with seven-transmembrane-domain glycoprotein receptors coupled to the G protein signaling pathway which selectively attract and activate different cell types (11). CXC chemokines represent a subfamily with first two of four invariant cysteine residues separated by a single amino acid and play an important role in regulation of angiogenesis, tumor immunity and organ specific metastasis (12, 13). CXC chemokine ligand-13 (CXCL13) which binds monogamously to the CXC chemokine receptor-5 (CXCR5) is involved in B-cell chemotaxis and is induced under inflammatory conditions (14). It has been shown that inflammatory cytokines such as interleukin (IL)-1β and TNF-α differentially modulate CXCL13 production in stromal and osteoblast cells derived from osteoarthritis patients (15). Similarly, IL-6 treatment significantly induced CXCL13 expression in human bone marrow endothelial cells and osteoblast cells, but not osteoclasts (16). Furthermore, HNSCC has been reported to predominantly express chemokine receptors such as CCR7 and CXCR5; however, CXCR4 expression is low or undetectable (17). Microarray analysis for gene expression profiling in OSCC identified high levels of CXCL13 expression, which is implicated in OSCC development and progression (18, 19). Recently, we showed nuclear factor of activated T-

cells, cytoplasmic 3 (NFATc3) is a downstream target of the CXCL13 signaling axis to stimulate RANKL expression in OSCC cells (20). Here, we report that CXCL13 activation of c-Myc induce RANKL expression in stromal/preosteoblast cells, which implicate CXCL13 as a potential therapeutic target to prevent OSCC invasion of bone/osteolysis.

Results

CXCL13 expression in primary human OSCC and bone marrow stromal/preosteoblast cells

We recently identified high levels of CXCL13 secretion in OSCC derived cell lines and further demonstrated a functional role in tumor invasion of bone/osteolysis in athymic mice (21). In this study, immunohistochemical staining using a tissue microarray (TMA) of sixty human OSCC tumors specimens identified > 95% of OSCC stained strong positive for CXCL13 expression; however a very low level expression was detected in normal adjacent tissue (Fig. 1A). We next measured the levels of CXCL13 in conditioned media (CM) obtained from the human bone marrow derived stromal cell line (SAKA-T) (22) and murine preosteoblast (MC3T3-E1) cells compared to OSCC tumor derived cell line (SCC-14a) by enzyme-linked immunosorbent assay (ELISA). We demonstrated SAKA-T and MC3T3-E1 cells produced very low levels (10 pg/ml) of CXCL13 compared to SCC-14a CM (120 pg/ml) (Fig. 1B). We then examined whether CXCL13 stimulates the CXCL13 specific receptor, CXCR5 expression in bone marrow stromal/preosteoblast cells. Western blot analysis of total cell lysates obtained from SAKA-T and MC3T3-E1 cells stimulated with CXCL13 (15 ng/ml) indicated a time-dependent increase in CXCR5 expression (Fig. 1C). These results suggest that OSCC secretion of CXCL13 at high levels modulates CXCR5 expression in stromal/preosteoblast cells.

CXCL13 stimulation of RANKL expression in stromal/preosteoblast cells

Previously we showed CXCL13 stimulation of RANKL, a critical osteoclastogenic factor expression in OSCC cells (20). We therefore examined the potential of OSCC CM to stimulate RANKL expression in bone marrow derived stromal/preosteoblast cells. Real-time reverse-transcription polymerase chain reaction (RT-PCR) analysis of total RNA isolated from MC3T3-E1 preosteoblast cells stimulated with CM (0–30%) obtained from OSCC cell lines (SCC-1, SCC-11B and SCC-14a) demonstrated a dose-dependent increase in RANKL mRNA expression. We further demonstrated that anti-CXCR5 antibody abolished SCC-14a CM (20%) and recombinant CXCL13 (15 ng/ml) induced RANKL expression in SAKA-T and MC3T3-E1 cells (Fig. 2A). In addition, cells stimulated with different concentrations (0–15 ng/ml) of CXCL13 revealed a dose-dependent increase in RANKL mRNA expression (Fig. 2B). Western blot analysis of total cell lysates obtained from SAKA-T, MC3T3-E1 and primary mouse bone marrow derived stromal cells further confirmed CXCL13 stimulation of RANKL expression (Fig. 2C). These results indicate that OSCC secretion of CXCL13 stimulates RANKL expression in stromal/preosteoblast cells.

CXCL13 transcriptional control of RANKL gene expression in stromal/preosteoblast cells

To determine the CXCL13 transcriptional control of RANKL expression, SAKA-T and MC3T3-E1 cells were transiently transfected with hRANKL-luciferase reporter plasmid (hRANKL P#3) by lipofectamine and treated with CXCL13 (0–15 ng/ml) for 6 h. Cells

mock-transfected with the empty vector (EV) served as controls. CXCL13 treatment dose-dependently increased the hRANKL gene promoter activity in SAKA-T and MC3T3-E1 cells (Fig. 3A&B). To further examine the CXCL13 transcriptional control of RANKL gene expression, we performed SuperArray screening for transcription factors. SAKA-T cells were stimulated with CXCL13 (15 ng/ml) for 6 h and total RNA isolated was used as template for SuperArray screening with real-time RT-PCR and data obtained were analyzed by a web portal as described in methods. We thus identified CXCL13 upregulation of c-Myc (4-fold) and NFATc3 (4.5-fold) transcription factors which have consensus binding motifs in the hRANKL promoter region (23) (data not shown). To further validate these results, total cell lysates obtained from MC3T3-E1 cells stimulated with different concentrations of CXCL13 (0–20 ng/ml) for 6 h were analyzed by Western blot. CXCL13 treatment resulted in a dose-dependent increase in c-Myc, NFATc3 and RANKL expression in these cells (Fig. 3C). We next examined the status of CXCL13 induced c-Myc activation in SAKA-T and MC3T3-E1 cells. As shown in Fig. 3D, cells stimulated with CXCL13 (15 ng/ml) for a variable period (0–60 min) had a significant increase in phospho-c-Myc (p-c-Myc) expression. Taken together, these data indicate that CXCL13 induction of c-Myc and NFATc3 transcription factors may upregulate RANKL gene expression in stromal/preosteoblast cells.

c-Myc activation in stromal/preosteoblast cells at OSCC tumor-bone interface

To determine the involvement of c-Myc and NFATc3 in OSCC tumor-bone microenvironment in vivo, we developed OSCC cells (SCC-11B) stably transfected with hRANKL-luciferase construct and injected (7×10^6 cells in PBS) subcutaneously onto the surface of calvaria in NCr-nu/nu athymic mice. Tumors appeared by day seven and thereafter continued to grow for five weeks period. Mice received D-luciferin (150 mg/kg, i.p) at weekly interval and bioluminescence signals were monitored as described in methods. OSCC tumors developed on calvaria demonstrated an increase in luciferase activity with tumor progression (Fig. 4A). Immunohistochemical analysis of OSCC tumors developed over calvaria in athymic mice demonstrated RANKL and NFATc3 expression in both tumor and osteoblast cells present at the tumor-bone interface. In contrast, p-c-Myc expression was detected only in osteoblastic cells. The osteoblastic cells in the tumor-bone interface were stained positive for alkaline phosphatase (ALP) activity (Fig. 4B). We then analyzed NFATc3 expression and c-Myc activation in primary human OSCC tumor specimens compared to normal adjacent tissue. Interestingly, immunohistochemical staining of human OSCC tumor specimens identified NFATc3 but not p-c-Myc expression. Furthermore, NFATc3 and p-c-Myc expression was not detected in normal adjacent tissue (Fig. 4C). These results suggest that c-Myc activation play an important role to modulate RANKL expression in stromal/preosteoblast cells in the OSCC tumor-bone microenvironment.

Functional role of c-Myc in CXCL13 stimulated RANKL expression in stromal/preosteoblast cells

Since c-Myc activation is specific to stromal/preosteoblast cells in the tumor-bone microenvironment, we next delineated the functional role of c-Myc in CXCL13 stimulation of RANKL expression in these cells. To assess the CXCL13-CXCR5 signaling axis operative in stromal/preosteoblast cells, SAKA-T and MC3T3-E1 cells were stimulated with

CXCL13 (15 ng/ml) for a variable period (0–60 min). Total cell lysates obtained were subjected to Western blot analysis to measure phospho-ERK1/2 (p-ERK1/2). As shown in Fig. 5A, CXCL13 stimulation significantly induced pERK1/2 expression in these cells in a time-dependent manner. Further, MC3T3-E1 cells were transfected with siRNA against NFATc3 or c-Myc by oligofectamine and stimulated with CXCL13 (15 ng/ml) for 48 h. Non-specific siRNA transfected cells served as control. Total cell lysates obtained were subjected to Western blot analysis for RANKL expression. MC3T3-E1 cells knock-down of NFATc3 demonstrated a significant decrease in RANKL; however no change in c-Myc expression (Fig. 5B). In contrast, MC3T3-E1 cells knock-down of c-Myc showed inhibition of both RANKL and NFATc3 expression (Fig. 5C). These results suggest that CXCL13 induced c-Myc expression is critical for NFATc3 regulation of RANKL expression in stromal/preosteoblast cells.

CXCL13 induced c-Myc nuclear translocation in preosteoblast cells

Because CXCL13 enhanced p-c-Myc expression in stromal/preosteoblast cells, we next examined the potential of CXCL13 induced p-c-Myc nuclear translocation in preosteoblast cells. MC3T3-E1 cells were stimulated with CXCL13 (15 ng/ml) for 6 h and immune stained with anti-p-c-Myc antibody. Confocal microscopy revealed that CXCL13 treatment induced nuclear translocation of p-c-Myc in these cells (Fig. 6A). We further analyzed c-Myc binding to the hRANKL gene promoter element via chromatin immunoprecipitation (ChIP) assay. SAKA-T cells stimulated with CXCL13 were analyzed by ChIP using anti-p-c-Myc antibody as described in methods. PCR analysis of chromatin immune complexes was then performed with hRANKL gene promoter specific primers. We identified that CXCL13 treatment significantly increased p-c-Myc binding to the RANKL promoter region. A low level of p-c-Myc binding in unstimulated cells could be due to basal level expression of CXCL13 produced by these cells (Fig. 6B&C). Collectively, these results suggest that CXCL13 activation of c-Myc induces RANKL expression in bone marrow stromal/preosteoblast cells.

Discussion

RANKL-RANK signaling is critical for osteoclast development and bone resorption activity (7). RANKL has been implicated as prognostic marker and therapeutic target for cancer metastasis (24–26). Also, CXCL13 has been identified as a prognostic marker in OSCC development (19). We demonstrated CXCL13 expression in primary human OSCC tumor specimens consistent with microarray profiling of gene expression in OSCC (18). In contrast to OSCC cells, stromal/preosteoblast cells produced low levels of CXCL13. However, human osteoblasts have been shown to express functional CXCR5 receptors (27). Our findings that OSCC production of CXCL13 which induces CXCR5 expression suggest a paracrine regulation in these cells. Furthermore, CXCL13 stimulation of RANKL expression in stromal/preosteoblast cells facilitates osteoclast activation and tumor invasion of bone/osteolysis. We recently identified elevated osteoclast formation/activity at OSCC tumor-bone microenvironment in athymic mice (21).

CXCL13 has been shown to be involved in prostate cancer progression and invasion through extracellular signal-regulated kinases (ERK) activation (28). Further, lipopolysaccharide treatment of osteoblasts induced RANKL expression in an ERK activation dependent manner (29). In addition, ERK signaling has been shown to promote c-Myc expression and activity in rhabdomyosarcoma tumor cells (30). Therefore, CXCL13 activation of ERK1/2 may play an important role in c-Myc and RANKL expression in stromal/preosteoblast cells. Tumor derived cytokines such as parathyroid hormone (PTH), IL-1β and prostaglandin E2 (PGE2) have been shown to up regulate RANKL expression in bone marrow stromal/ osteoblast cells (31–33). Furthermore, OSCC production of osteotropic cytokines and stimulation of stromal cells to synthesize IL-6 in the tumor-bone microenvironment favors osteoclast formation/activation (34). Therefore, it is possible that OSCC production of osteotropic cytokines regulate RANKL expression independent of the CXCL13-CXCR5 signaling axis in stromal/preosteoblast cells. However, CXCL13 up regulation of hRANKL promoter activity in stromal/preosteoblast cells indicate CXCL13-CXCR5 signaling axis transcriptionally modulate RANKL expression in these cells. Our results that superarray screening identified CXCL13 upregulation of c-Myc and NFATc3 which has consensus binding motifs in the hRANKL promoter region and ChIP assay demonstrated p-c-Myc binding to the hRANKL promoter region further confirms the CXCL13 transcriptional control of RANKL expression.

It has been demonstrated that increased RANKL expression in stromal cells results in excess bone resorption in multiple myeloma (35). Also, RANKL expression in fibroblastic cells in human gingival squamous cell carcinomas is implicated in bone invasion (36). In addition, prostate tumor cells and osteoclast production of MMP-7 has been shown to contribute to tumor induced osteolysis through solubilization of RANKL in the tumor-bone microenvironment (37). Similarly, tumor cell interaction with osteoclasts results in up regulation of cathepsin G expression which promotes tumor osteolysis through solubilization of RANKL (38). Therefore, OSCC production of matrix metalloproteases may increase soluble RANKL which promote tumor invasion of bone. This study further identify that CXCL13 induces c-Myc and NFATc3 expression in stromal/preosteoblast cells; however, c-Myc activation is specific in preosteoblast cells at the tumor-bone interface. Variable levels of c-Myc expression has been reported in OSCC tumors at different stages (39). In this study, we observe lack of c-Myc activation in primary OSCC specimens from human subjects and mouse xenograft model. NFATc1 regulate c-Myc gene transcription in pancreatic cancer cells (40). Conversely, c-Myc expression has been shown to increase intracellular calcium levels and NFAT activation in B lymphocytes (41). Also, sequential induction of NFAT and c-Myc by TGF-β promote cancer cell proliferation (42). In this study, we show that siRNA suppression of c-Myc inhibits CXCL13 induced NFATc3 and RANKL expression indicates that c-Myc activation is critical for RANKL expression in stromal/preosteoblast cells. Thus, our findings are novel that CXCL13 production by OSCC cells stimulates RANKL expression in bone marrow stromal/preosteoblast cells and c-Myc is a downstream target of the CXCL13/CXCR5 axis to stimulate RANKL expression. Collectively, our studies implicate CXCL13 as a potential therapeutic target to prevent OSCC invasion of bone/osteolysis.

Materials and Methods

Reagents and Antibodies

Cell culture and DNA transfection reagents were purchased from Invitrogen (Carlsbad, CA). E.coli derived recombinant human CXCL13 (purity >95%), anti-CXCR5, anti-human RANKL antibodies and CXCL13 ELISA kits were purchased from R&D systems Inc (Minneapolis, MN). Anti- NFATc3, anti-c-Myc, anti-ERK, anti-p-ERK, peroxidase-conjugated secondary antibodies and siRNA against NFATc3 and c-Myc were purchased from Santa Cruz Biotechnology, CA. Anti-p-c-Myc was purchased from Cell Signaling Technology Inc (Danvers, MA). Super signal-enhanced chemiluminescence (ECL) system (Pierce, Rockford, IL) and PVDF membranes were purchased from Millipore (Bedford, MA). A luciferase reporter assay system was obtained from Promega (Madison, WI) and protease inhibitor cocktail was purchased from Sigma (St. Louis, MO).

OSCC cell culture

Human OSCC tumor-derived SCC-1, SCC-11B and SCC-14a cell lines (43) were cultured in DMEM supplemented with 10% fetal bovine serum and 100 units/ml penicillin/streptomycin in a humidified atmosphere with 5% CO_2 at 37°C. In sub-confluent state, cells were washed twice with PBS and once with serum-free DMEM, and subsequently cultured in serum-free DMEM for 24 h. The conditioned media (CM) collected was centrifuged to eliminate intact cells, debris and stored at −80 °C for further use.

Bioluminescence Imaging

SCC-11B cells (7×10^6) stably transfected with RANKL-luciferase construct were injected subcutaneously (n=10) in phosphate buffered saline (PBS) overlaying the calvaria of NCr-nu/nu athymic mice, aged 4 to 6 weeks (NCI, Frederick, MD) and PBS alone injected were served as control group (n=8). At the end of experimental period, mice received D-luciferin (150 mg/kg, i.p) under 1–2% inhaled isoflurane anesthesia. The bioluminescence signals were monitored using the IVIS system 200 series consisting of a highly sensitive cooled CCD camera and Living Image software (Xenogen Corp., USA) was used to grid the imaging data and integrates the total bioluminescence signals in each boxed region. Two kinetic bioluminescent acquisitions were collected between 0 and 20 min after D-luciferin injection to confirm the peak photon emission recorded as maximum photon efflux per second. All fluorescence images were acquired with a 15 s exposure. Data were analyzed using the total photon flux emission (photons/second) in the regions of interest covering the entire calvarial region. All the animal procedures were performed following the Institutional Animal Care and Use Committee (IACUC) approved protocol.

Quantification of CXCL13

CXCL13 levels in serum free conditioned media (CM) from SCC-14a, human bone marrow derived stromal cell line (SAKA-T) and mouse preosteoblast cell line (MC3T3-E1) was measured using the human and mouse specific ELISA kits (R&D systems, Minneapolis, MO) following the manufacturer's protocol.

Immunohistochemistry

Tissue microarray (TMA) of sixty primary human OSCC tumors specimens were obtained from the Head and Neck Cancer Tissue Array Initiative at the NIDCR, NIH (44) and eight control adjacent normal tissues were obtained from the Hollings Cancer Center Tissue Biorepository in accordance with an Institutional Review Board (IRB) approved protocol. Formalin-fixed OSCC tumor specimens from athymic mice or human subjects were processed for paraffin sectioning. Serial 5-μm sections were cut on a modified Leica RM 2155 rotary microtome (Leica Microsystems, Ontario, Canada). Antigen retrieval was performed with Target Retrieval Solution (DAKO, Carpinteria, CA) coupled with steaming. The slides were incubated with primary anti-CXCL13, anti-NFATc3, anti-RANKL and anti-p-c-Myc antibodies for 60 min at room temperature. Immunohistochemical staining was performed with HRP labeled secondary antibody and DAB (Vector Laboratories, Burlingame, CA). The slides were briefly counterstained with hematoxylin, and dehydrated through graded alcohols to xylene and were cover slipped with a permanent mounting media.

Quantitative Real-Time RT-PCR

RANKL mRNA expression levels were measured by real-time RT-PCR as described earlier (20). Briefly, total RNA was isolated from SAKA-T and MC3T3-E1 cells treated with/without different concentrations of conditioned media (0–30%) obtained from OSCC cell lines or recombinant CXCL13 (0–15 ng/ml) for 6 h using RNAzol reagent (Biotecx Labs, Houston, TX). To eliminate the residual genomic DNA contamination, total RNA was treated with DNAse I (Sigma) at room temperature for 15 min followed by 10 min at 65 °C with the addition of 25 mM EDTA. The RNA integrity of samples was evaluated based on the intensity of 28S and 18S rRNA bands on agarose gels and A_{260}/A_{280} ratio between 1.8 and 2.0. The reverse transcription reaction was performed using poly-dT primer and Moloney murine leukemia virus reverse transcriptase (Applied Biosystems, Foster City, CA) in a 25 μl reaction volume containing total RNA (2 μg), 1× PCR buffer and 2 mM $MgCl_2$, at 42 °C for 15 min followed by 95 °C for 5 min. The quantitative real-time RT-PCR was performed using IQ™ SYBR Green Supermix in an iCycler (iCycler iQ Single-color real-time-PCR detection system; Bio-Rad, Hercules, CA). The primer sequences used to amplify human glyceraldehyde-3-phosphate dehydrogenase (hGAPDH) mRNA were 5′-CCTACCCCCAATGTATCCGTTGTG-3 (sense) and 5′-GGAGGAATGGGAGTTGCTGTTGAA-3′ (anti-sense); hRANKL mRNA 5′-ACCAGCATCAAAATCCCAAG-3′ (sense) and 5′-TAAGGAGTTGGAGACCT-3′ (anti-sense). The primers to amplify mGAPDH mRNA were 5′-ACC ACA GTC CAT GCC ATC AC -3 (sense) and 5′-TCC ACC ACC CTG TTG CTG TA-3′ (anti-sense); mRANKL mRNA 5′-CAG CCA TTT GCA CAC CTC ACC ATC-3′ (sense) and 5′-TTT CGT GCT CCC TCC TTT CAT CAG-3′ (anti-sense). Thermal cycling parameters were 94 °C for 3 min, followed by 35 cycles of amplifications at 94 °C for 30 s, 60 °C for 1 min, 72 °C for 2 min, and 72 °C for 10 min as the final elongation step. The melt curve analysis was performed from 59–95 °C with 0.5 °C increments. The specificities of PCR amplifications were assessed from the melt curves to confirm the presence of gene specific peaks. Relative

levels of mRNA expression were normalized in all the samples analyzed with respect to the levels of GAPDH amplification.

hRANKL Promoter-Luciferase Reporter Gene Assay

SAKA-T cells were cultured in α-MEM and MC3T3-E1 cells were cultured in α-MEM containing ribonucleosides and deoxyribonucleosides without ascorbic acid. The media were supplemented with 10% fetal bovine serum (FBS), 100 units/ml penicillin/streptomycin and cells were cultured in a humidified atmosphere with 5% CO_2 at 37 °C. hRANKL promoter-luciferase reporter plasmid (hRANKL P#3) construct (23) was transiently transfected into SAKA-T and MC3T3-E1 cells using lipofectamine. The transfection efficiency was normalized by co-transfection with 0.2 μg of pRSV β-gal plasmid and β-galactosidase activity was measured in the cells (Promega, Madison, WI). LacZ cytochemical activity staining (Invitrogen, Inc., San Diego, CA) indicated the DNA transfection efficiency >80% in these cells. Cells were stimulated with *E. coli* expressed recombinant hCXCL13 (0–15 ng/ml) for 6 h. Cell monolayer was washed twice with phosphate buffered saline and incubated at room temperature for 15 min with 0.3 ml cell lysis reagent. A 20 μl aliquot of each sample was mixed with 100 μl of the luciferase assay reagent. The light emission was measured for 10 s of integrated time using a Sirius Luminometer following the manufacturer's instructions (Promega, Madison, WI)

Western Blot Analysis

SAKA-T and MC3T3-E1 cells were seeded (5×10^5 cells/well) in 6-well plates and supplemented with α-MEM containing 10% FBS. Cells were stimulated with or without CXCL13 as indicated and total cell lysates were prepared in a buffer containing 20 mM Tris-HCl at pH 7.4, 1% Triton X-100, 1 mM EDTA, 1.5 mM $MgCl_2$, 10% glycerol, 150 mM NaCl, 0.1 mM Na_3VO_4 and 1× protease inhibitor cocktail. The protein content of the samples was measured using the BCA protein assay reagent (Pierce, Rockford, IL). Protein (100 μg) samples were then subjected to SDS-PAGE using 4–15% Tris-HCl gels and blot transferred on to a PVDF membrane and immunoblotted with anti-CXCR5, anti-RANKL, anti-c-Myc, anti-p-c-Myc, anti-NFATc3 and anti-ERK/p-ERK antibodies. The bands were detected using the enhanced chemiluminescence detection system. The band intensity was quantified by densitometric analysis using the NIH ImageJ Program.

SuperArray Screening

SAKA-T cells (5×10^6 cells/well) were cultured in a 60 mm tissue culture plate with or without CXCL13 (15 ng/ml) for 6 h and total RNA was isolated using RNAzol reagent. Reverse transcription reaction was performed as described earlier. Real-time PCR was performed using 2x SuperArray RT qPCR Master Mix (RT^2 Profiler™ PCR Array System (SuperArray PAHS-075A-02) in a 96-well plate to quantify expression levels of 84 transcription factors. Thermal cycling parameters were 95 °C for 10 min, followed by 40 cycles of amplifications at 95 °C for 15 s, 55 °C for 30 s, 72 °C for 30 s, and 72 °C for 5 min as the final elongation step. Relative mRNA expression was normalized in all samples with housekeeping gene expression, and data analysis was performed using the web portal (www.superarray.com/pcrarraydataanalysis.php).

Confocal Microscopy

MC3T3-E1 cells were cultured (1×10^3/well) in a Lab-Tek 4-well chamber slides (Nunc Inc, Rochester, NY). Cells were stimulated with and without CXCL13 (15 ng/ml) for 6 h and fixed with 4% paraformaldehyde in PBS for 10 min at room temperature. Cells were permeabilized with 0.1% Triton X-100 for 10 min and blocked for 1 h with PBS containing 2% horse serum at room temperature. Cells were incubated with rabbit anti-p-c-Myc (10 μg/ml) antibody for 3 h and treated with Alexa 488-conjugated anti-rabbit IgG in PBS containing 2% horse serum for 1 h at room temperature. The nuclear staining was performed with DRAQ5 and cellular localization of p-c-Myc was visualized by confocal microscopy (LSM 510; Carl Zeiss, Inc., Thornwood, NY).

Chromatin Immunoprecipitation (ChIP) Assay

ChIP was performed using the ChIP Assay Kit (Upstate, Temecula, CA) following the manufacturer's instructions. Briefly, human bone marrow derived stromal cells (SAKA-T) were stimulated with and without CXCL13 (15 ng/ml) for 6 h. Cells were cross-linked with 1% formaldehyde for 10 min. Soluble chromatin was prepared by sonication using the Branson-250 digital sonifier (Branson Ultrasonics, Danbury, CT) to an average DNA length of 200–1,000 bp. Approximately 5×10^5 cell equivalent (1/6th) of the sheared soluble chromatin was precleared with blocked Protein G agarose, and 10% of the precleared chromatin was set aside as input control. Immunoprecipitation was carried out with anti-p-c-Myc antibody (5 μg) or equivalent concentrations of rabbit IgG as negative control overnight at 4 °C. Immune complexes were pulled down using Protein G agarose, washed and eluted twice with 250 μl of elution buffer (0.1 M $NaHCO_3$, 1% SDS) and cross-linking reversed in 200 mM NaCl at 65 °C overnight with 20 μg RNase A. DNA was purified following proteinase K treatment with the Qiagen PCR purification kit (Qiagen, MD). To analyze the p-c-Myc binding to the hRANKL gene promoter region, the immunoprecipitated chromatin DNA samples were subjected to PCR analysis using primer pairs to amplify c-Myc binding region (−1393 bp to −1388 bp) in the hRANKL promoter (23): 5′-ATT TAG AAC ACA TGC TTT AAT A-3′ (sense) and 5′-TGC CTA ATT CGC TAA TGA GTA TTT C-3′ (anti-sense). Thermal cycling parameters of a 20 μl reaction mixture were 94 °C for 30 s, followed by 35 cycles of amplifications at 94 °C for 30 s, 55 °C for 30 s, 72 °C for 30 s, and 72 °C for 5 min as the final elongation step. PCR products were electrophoresed on 2% agarose gels and visualized by ethidium bromide.

siRNA Interference

MC3T3-E1 cells were seeded (5×10^5 cells/well) in 6-well plates and supplemented with α-MEM containing 10% FBS. One day after seeding, cells were transfected with double-stranded siRNA (20 nM) against NFATc3 or c-Myc by oligofectamine for 48 h. Non-specific siRNA transfected cells served as control. Cells were cultured in the presence and absence of CXCL13 (15 ng/ml) for 6 h. Total cell lysates obtained were analyzed by Western blot for RANKL, c-Myc and NFATc3 expression using specific antibodies.

Statistical Analysis

Results are presented as mean ± SD for three independent experiments and compared by Student 't'-test. Values were considered significant at *p< 0.05.

Acknowledgments

We thank Dr. Thomas E. Carey, University of Michigan, Ann Arbor, MI for generously providing OSCC cells and Alfredo A. Molinolo M.D., Ph.D, NIDCR, NIH for providing the OSCC tumor tissue microarray slides. This work was conducted in a facility constructed with support from the National Institutes of Health, Grant Number C06 RR015455 from the Extramural Research Facilities Program of the National Center for Research Resources.

References

1. Mao L, Hong WK, Papadimitrakopoulou VA. Focus on head and neck cancer. Cancer Cell. 2004; 5:311–316. [PubMed: 15093538]
2. Funk GF, Karnell LH, Robinson RA, Zhen WK, Trask DK, Hoffman HT. Presentation, treatment, and outcome of oral cavity cancer: a National Cancer Data Base report. Head Neck. 2002; 24:165–180. [PubMed: 11891947]
3. Choi S, Myers JN. Molecular pathogenesis of oral squamous cell carcinoma: implications for therapy. J Dent Res. 2008; 87:14–32. [PubMed: 18096889]
4. Nomura T, Shibahara T, Katakura A, Matsubara S, Takano N. Establishment of a murine model of bone invasion by oral squamous cell carcinoma. Oral Oncol. 2007; 43:257–262. [PubMed: 16920384]
5. Mishra A, Bharti AC, Varghese P, Saluja D, Das BC. Differential expression and activation of NF-kappaB family proteins during oral carcinogenesis: Role of high risk human papillomavirus infection. Int J Cancer. 2006; 119:2840–2850. [PubMed: 16998793]
6. Uchida D, Kawamata H, Omotehara F, Nakashiro K, Kimura-Yanagawa T, Hino S, et al. Role of HGF/c-met system in invasion and metastasis of oral squamous cell carcinoma cells in vitro and its clinical significance. Int J Cancer. 2001; 93:489–496. [PubMed: 11477552]
7. Hsu H, Lacey DL, Dunstan CR, Solovyev I, Colombero A, Timms E, et al. Tumor necrosis factor receptor family member RANK mediates osteoclast differentiation and activation induced by osteoprotegerin ligand. Proc Natl Acad Sci USA. 1999; 96:3540–3545. [PubMed: 10097072]
8. Deyama Y, Tei K, Yoshimura Y, Izumiyama Y, Takeyama S, Hatta M, et al. Oral squamous cell carcinomas stimulate osteoclast differentiation. Oncol Rep. 2008; 20:663–668. [PubMed: 18695921]
9. Lynch CC, Hikosaka A, Acuff HB, Martin MD, Kawai N, Singh RK, et al. MMP-7 promotes prostate cancer-induced osteolysis via the solubilization of RANKL. Cancer Cell. 2005; 7:485–496. [PubMed: 15894268]
10. Jimi E, Furuta H, Matsuo K, Tominaga K, Takahashi T, Nakanishi O. The cellular and molecular mechanisms of bone invasion by oral squamous cell carcinoma. Oral Dis. 2011; 17:462–468. [PubMed: 21496184]
11. Zlotnik A, Yoshie O. Chemokines: a new classification system and their role in immunity. Immunity. 2000; 12:121–127. [PubMed: 10714678]
12. Belperio JA, Keane MP, Arenberg DA, Addison CL, Ehlert JE, Burdick MD, et al. CXC chemokines in angiogenesis. J Leukoc Biol. 2000; 68:1–8. [PubMed: 10914483]
13. Muller A, Homey B, Soto H, Ge N, Catron D, Buchanan ME, et al. Involvement of chemokine receptors in breast cancer metastasis. Nature. 2001; 410:50–56. [PubMed: 11242036]
14. Legler DF, Loetscher M, Roos RS, Clark-Lewis I, Baggiolini M, Moser B. B cell-attracting chemokine 1, a human CXC chemokine expressed in lymphoid tissues, selectively attracts B lymphocytes via BLR1/CXCR5. J Exp Med. 1998; 187:655–660. [PubMed: 9463416]
15. Lisignoli G, Cristino S, Toneguzzi S, Grassi F, Piacentini A, Cavallo C, et al. IL1beta and TNFalpha differently modulate CXCL13 chemokine in stromal cells and osteoblasts isolated from

osteoarthritis patients: evidence of changes associated to cell maturation. Exp Gerontol. 2004; 39:659–665. [PubMed: 15050303]

16. Singh S, Singh R, Sharma PK, Singh UP, Rai SN, Chung LW, et al. Serum CXCL13 positively correlates with prostatic disease, prostate-specific antigen and mediates prostate cancer cell invasion, integrin clustering and cell adhesion. Cancer Lett. 2009; 283:29–35. [PubMed: 19375853]
17. Muller A, Sonkoly E, Eulert C, Gerber PA, Kubitza R, Schirlau K, et al. Chemokine receptors in head and neck cancer: association with metastatic spread and regulation during chemotherapy. Int J Cancer. 2006; 118:2147–2157. [PubMed: 16331601]
18. Ziober AF, Patel KR, Alawi F, Gimotty P, Weber RS, Feldman MM, et al. Identification of a gene signature for rapid screening of oral squamous cell carcinoma. Clin Cancer Res. 2006; 12:5960–5971. [PubMed: 17062667]
19. Vachani A, Nebozhyn M, Singhal S, Alila L, Wakeam E, Muschel R, et al. A 10-gene classifier for distinguishing head and neck squamous cell carcinoma and lung squamous cell carcinoma. Clin Cancer Res. 2007; 13:2905–2915. [PubMed: 17504990]
20. Yuvaraj S, Griffin AC, Sundaram K, Kirkwood KL, Norris JS, Reddy SV. A Novel Function of CXCL13 to Stimulate RANK Ligand Expression in Oral Squamous Cell Carcinoma Cells. Mol Cancer Res. 2009; 7:1399–1407. [PubMed: 19671684]
21. Pandruvada SN, Yuvaraj S, Liu X, Sundaram K, Shanmugarajan S, Ries WL, et al. Role of CXC chemokine ligand 13 in oral squamous cell carcinoma associated osteolysis in athymic mice. Int J Cancer. 2010; 126:2319–2329. [PubMed: 19816883]
22. Darimont C, Avanti O, Tromvoukis Y, Vautravers-Leone P, Kurihara N, Roodman GD, et al. SV40 T antigen and telomerase are required to obtain immortalized human adult bone cells without loss of the differentiated phenotype. Cell Growth Differ. 2002; 13:59–67. [PubMed: 11864909]
23. Roccisana JL, Kawanabe N, Kajiya H, Koide M, Roodman GD, Reddy SV. Functional role for heat shock factors in the transcriptional regulation of human RANK ligand gene expression in stromal/osteoblast cells. J Biol Chem. 2004; 279:10500–10507. [PubMed: 14699143]
24. Chen G, Sircar K, Aprikian A, Potti A, Goltzman D, Rabbani SA. Expression of RANKL/RANK/OPG in primary and metastatic human prostate cancer as markers of disease stage and functional regulation. Cancer. 2006; 107:289–298. [PubMed: 16752412]
25. Mikami S, Katsube K, Oya M, Ishida M, Kosaka T, Mizuno R, et al. Increased RANKL expression is related to tumour migration and metastasis of renal cell carcinomas. J Pathol. 2009; 218:530–539. [PubMed: 19455604]
26. Tan W, Zhang W, Strasner A, Grivennikov S, Cheng JQ, Hoffman RM, et al. Tumour-infiltrating regulatory T cells stimulate mammary cancer metastasis through RANKL-RANK signalling. Nature. 2011; 470:548–553. [PubMed: 21326202]
27. Lisignoli G, Toneguzzi S, Piacentini A, Cattini L, Lenti A, Tschon M, et al. Human osteoblasts express functional CXC chemokine receptors 3 and 5: activation by their ligands, CXCL10 and CXCL13, significantly induces alkaline phosphatase and beta-N-acetylhexosaminidase release. J Cell Physiol. 2003; 194:71–79. [PubMed: 12447991]
28. El-Haibi CP, Singh R, Sharma PK, Singh S, Lillard JW Jr. CXCL13 mediates prostate cancer cell proliferation through JNK signalling and invasion through ERK activation. Cell Prolif. 2011; 44:311–319. [PubMed: 21645150]
29. Kikuchi T, Yoshikai Y, Miyoshi J, Katsuki M, Musikacharoen T, Mitani A, et al. Cot/Tpl2 is essential for RANKL induction by lipid A in osteoblasts. J Dent Res. 2003; 82:546–550. [PubMed: 12821717]
30. Marampon F, Ciccarelli C, Zani BM. Down-regulation of c-Myc following MEK/ERK inhibition halts the expression of malignant phenotype in rhabdomyosarcoma and in non muscle-derived human tumors. Mol Cancer. 2006; 5:31. [PubMed: 16899113]
31. Hofbauer LC, Heufelder AE. Role of receptor activator of nuclear factor-kappaB ligand and osteoprotegerin in bone cell biology. J Mol Med. 2001; 79:243–253. [PubMed: 11485016]
32. Lee SK, Kalinowski J, Jastrzebski S, Lorenzo JA. 1,25(OH)2 vitamin D3-stimulated osteoclast formation in spleen-osteoblast cocultures is mediated in part by enhanced IL-1 alpha and receptor

activator of NF-kappa B ligand production in osteoblasts. J Immunol. 2002; 169:2374–2380. [PubMed: 12193704]

33. Nakashima T, Kobayashi Y, Yamasaki S, Kawakami A, Eguchi K, Sasaki H, et al. Protein expression and functional difference of membrane-bound and soluble receptor activator of NF-kappaB ligand: modulation of the expression by osteotropic factors and cytokines. Biochem Biophys Res Commun. 2000; 275:768–775. [PubMed: 10973797]
34. Kayamori K, Sakamoto K, Nakashima T, Takayanagi H, Morita K, Omura K, et al. Roles of interleukin-6 and parathyroid hormone-related peptide in osteoclast formation associated with oral cancers: significance of interleukin-6 synthesized by stromal cells in response to cancer cells. Am J Pathol. 2010; 176:968–980. [PubMed: 20035059]
35. Roux S, Mariette X. The high rate of bone resorption in multiple myeloma is due to RANK (receptor activator of nuclear factor-kappaB) and RANK Ligand expression. Leuk Lymphoma. 2004; 45:1111–1118. [PubMed: 15359989]
36. Ishikuro M, Sakamoto K, Kayamori K, Akashi T, Kanda H, Izumo T, et al. Significance of the fibrous stroma in bone invasion by human gingival squamous cell carcinomas. Bone. 2008; 43:621–627. [PubMed: 18585993]
37. Thiolloy S, Halpern J, Holt GE, Schwartz HS, Mundy GR, Matrisian LM, et al. Osteoclast-derived matrix metalloproteinase-7, but not matrix metalloproteinase-9, contributes to tumor-induced osteolysis. Cancer Res. 2009; 69:6747–6755. [PubMed: 19679556]
38. Wilson TJ, Nannuru KC, Futakuchi M, Sadanandam A, Singh RK. Cathepsin G enhances mammary tumor-induced osteolysis by generating soluble receptor activator of nuclear factor-kappaB ligand. Cancer Res. 2008; 68:5803–5811. [PubMed: 18632634]
39. Perez-Sayans M, Suarez-Penaranda JM, Pilar GD, Barros-Angueira F, Gandara-Rey JM, Garcia-Garcia A. What real influence does the proto-oncogene c-myc have in OSCC behavior? Oral Oncol. 2011; 47:688–692. [PubMed: 21708481]
40. Buchholz M, Schatz A, Wagner M, Michl P, Linhart T, Adler G, et al. Overexpression of c-myc in pancreatic cancer caused by ectopic activation of NFATc1 and the Ca2+/calcineurin signaling pathway. EMBO J. 2006; 25:3714–3724. [PubMed: 16874304]
41. Habib T, Park H, Tsang M, de Alboran IM, Nicks A, Wilson L, et al. Myc stimulates B lymphocyte differentiation and amplifies calcium signaling. J Cell Biol. 2007; 179:717–731. [PubMed: 17998397]
42. Singh G, Singh SK, Konig A, Reutlinger K, Nye MD, Adhikary T, et al. Sequential activation of NFAT and c-Myc transcription factors mediates the TGF-beta switch from a suppressor to a promoter of cancer cell proliferation. J Biol Chem. 2010; 285:27241–27250. [PubMed: 20516082]
43. Brenner JC, Graham MP, Kumar B, Saunders LM, Kupfer R, Lyons RH, et al. Genotyping of 73 UM-SCC head and neck squamous cell carcinoma cell lines. Head Neck. 2010; 32:417–426. [PubMed: 19760794]
44. Molinolo AA, Hewitt SM, Amornphimoltham P, Keelawat S, Rangdaeng S, Meneses Garcia A, et al. Dissecting the Akt/mammalian target of rapamycin signaling network: emerging results from the head and neck cancer tissue array initiative. Clin Cancer Res. 2007; 13:4964–4973. [PubMed: 17785546]

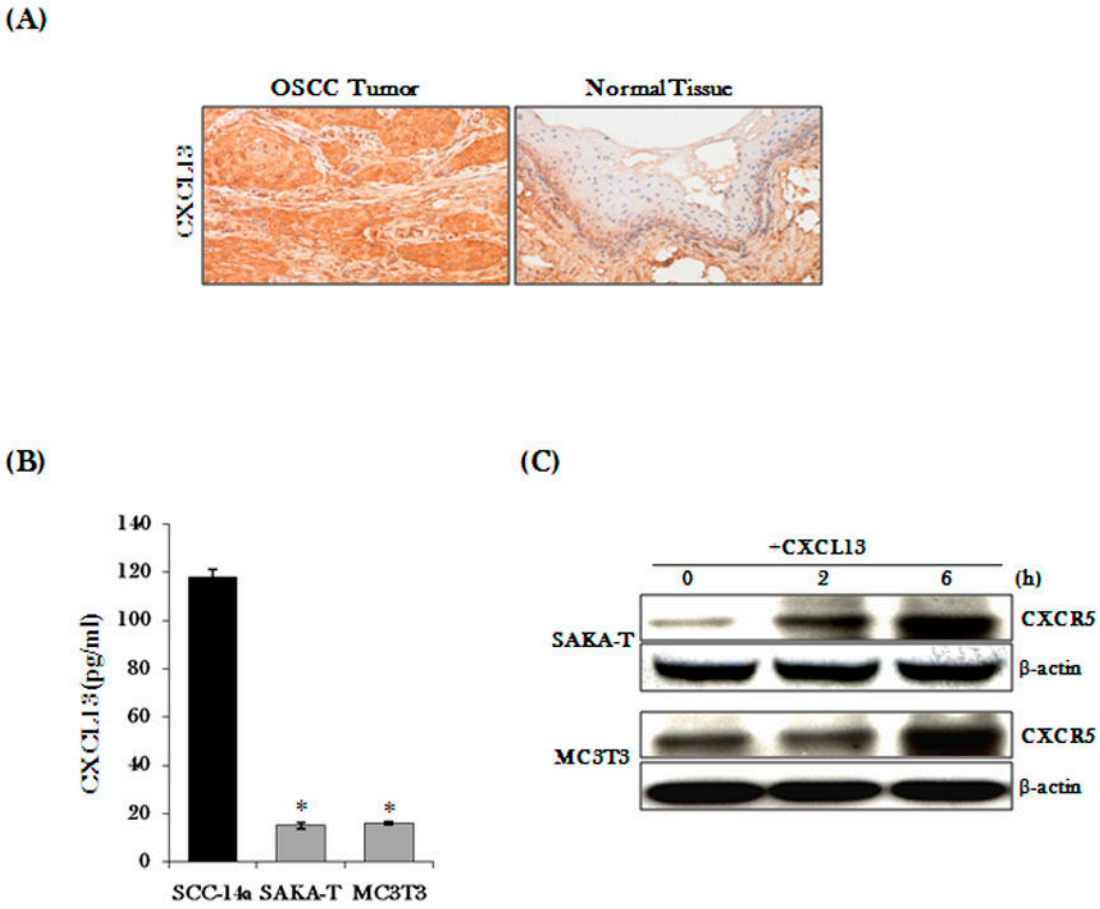

Figure 1.

CXCL13 expression in OSCC, stromal/preosteoblast cells. (A) Representative sections showing immunohistochemical staining for CXCL13 expression in OSCC tumor specimens and control adjacent normal tissues from human subjects. (B) CXCL13 levels in serum free conditioned media (CM) obtained from SCC-14a, human bone marrow derived stromal cells (SAKA-T) and murine preosteoblast cells (MC3T3-E1) as measured by ELISA. (C) CXCL13 stimulation of CXCR5 receptor expression in bone marrow stromal/preosteoblast cells. SAKA-T and MC3T3-E1 cells were treated with recombinant CXCL13 (15 ng/ml) for 0–6 h and the total cell lysates were analyzed for CXCR5 expression by Western blot. β-actin expression served as control. Data represent three replicate studies (*$p<0.05$).

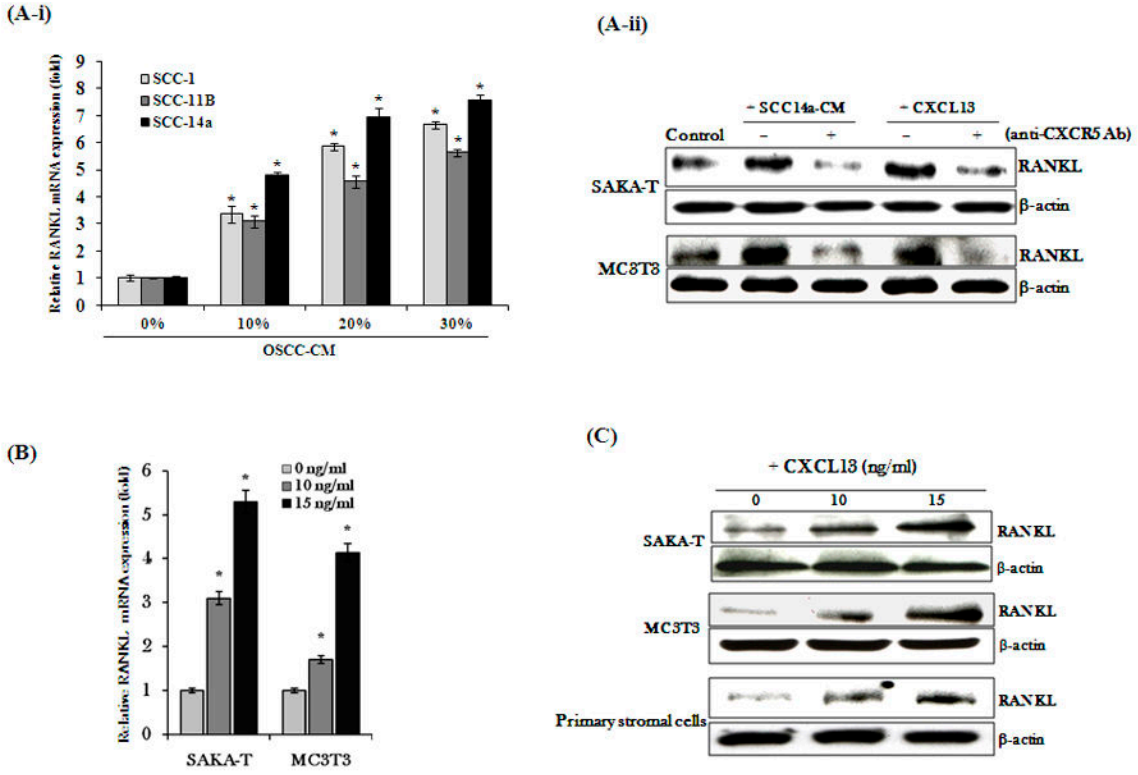

Figure 2.

CXCL13 stimulation of RANKL expression in stromal/preosteoblast cells. (A-i) Real time RT-PCR analysis for RANKL mRNA expression in MC3T3-E1 preosteoblast cells stimulated with CM (0–30%) obtained from different OSCC cell lines (SCC-1, SCC-11B and SCC-14a). (A-ii) SCC-14a cell CM stimulates RANKL expression in stromal/ preosteoblast cells. Human bone marrow derived stromal cells (SAKA-T) and murine preosteoblast cells (MC3T3-E1) were stimulated with SCC-14a CM (20%) or recombinant CXCL13 (15 ng/ml) in the presence and absence of anti-CXCR5 antibody (10 μg/ml) for 6 h. The total cell lysates were subjected to Western blot analysis for RANKL expression. (B) CXCL13 stimulation of RANKL mRNA expression in SAKA-T and MC3T3-E1 cells. Cells were stimulated with CXCL13 (15 ng/ml) and total RNA isolated from these cells were analyzed for RANKL mRNA expression by Real-time RT-PCR. The relative mRNA expression was normalized with respect to GAPDH amplification. The values are expressed as mean ± SD (*$p<0.05$). (C) CXCL13 dose-dependent stimulation of RANKL expression in SAKA-T, MC3T3-E1 and mouse bone marrow derived primary stromal cells. Cells were treated with different concentrations (0–15 ng/ml) of CXCL13 for 6 h and total cell lysates were analyzed for RANKL expression by Western blot. β-actin expression serves as control. Data shown are representative of three replicate studies.

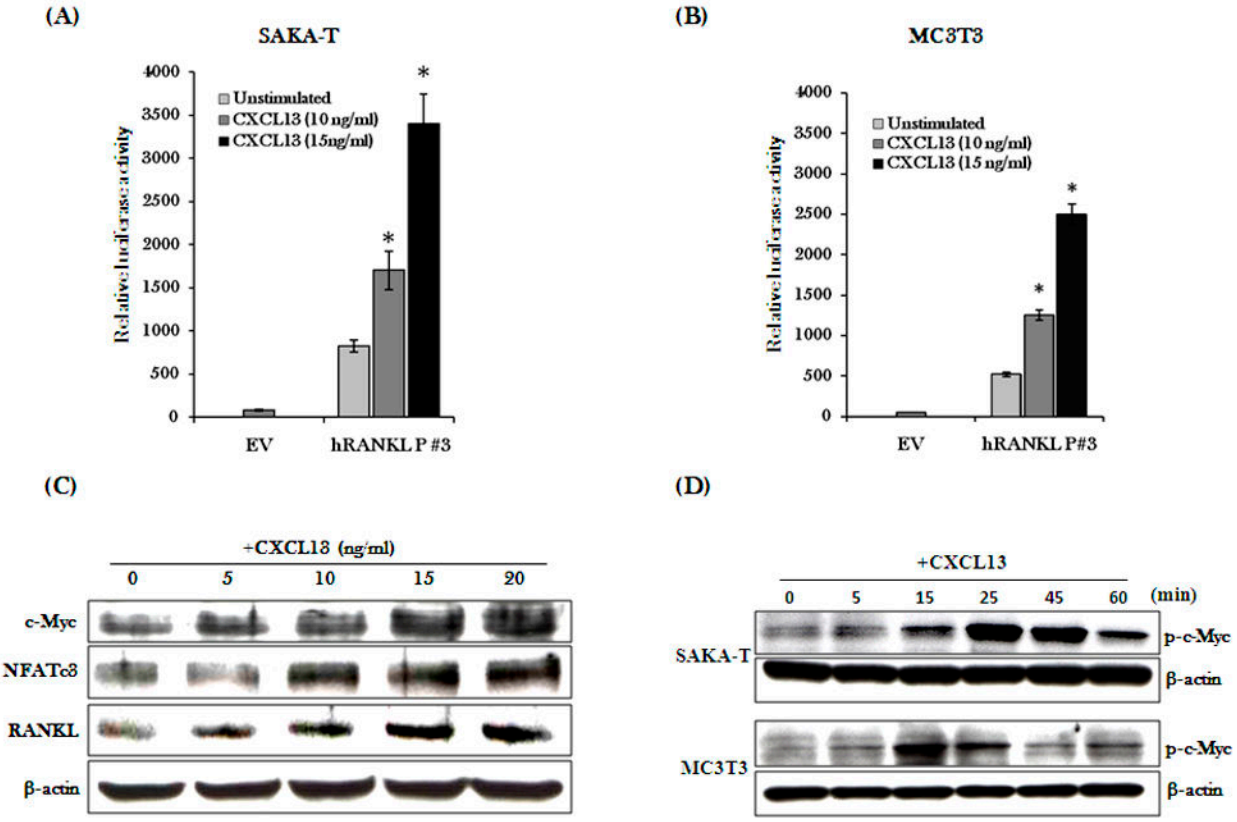

Figure 3.

CXCL13 transcriptional control of RANKL expression in human bone marrow derived stromal cells (SAKA-T) and murine preosteoblast (MC3T3-E1) cells. (A) SAKA-T and (B) MC3T3-E1 cells were transiently transfected with hRANKL-luc P#3 plasmid by lipofectamine and cultured with CXCL13 (0–15 ng/ml) for 6 h. Cells mock-transfected with empty vector (EV) served as control. Total cell lysates prepared were assayed for luciferase activity. (C) MC3T3-E1 cells were treated with different concentrations of recombinant CXCL13 (0–20 ng/ml) for 6 h. Total cell lysates obtained were analyzed for c-Myc, NFATc3 and RANKL expression by Western blot. (D) CXCL13 activation of c-Myc in SAKA-T and MC3T3-E1 cells. Cells were treated with CXCL13 (15 ng/ml) for 0–60 min and total cell lysates obtained were analyzed for p-c-Myc by Western blot. β-actin expression served as control. Data represent three replicate studies and mean ± SD (*$p<0.05$).

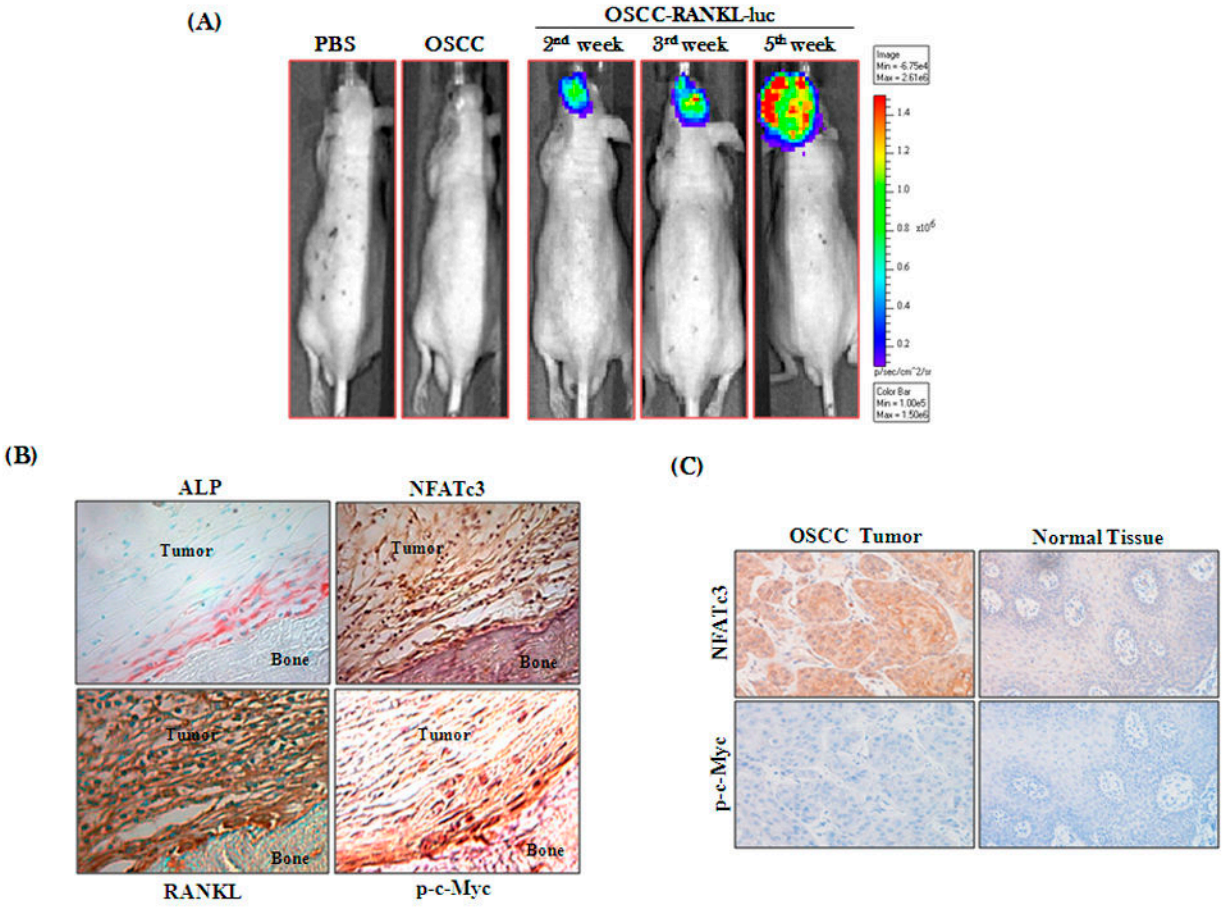

Figure 4.

RANKL, p-c-Myc, NFATc3 expression in OSCC tumor-bone microenvironment. (A) OSCC tumor progression in athymic mice. NCr-nu/nu athymic mice were subcutaneously injected with SCC-11B cells (7×10^6) with or without stable RANKL-Luc reporter gene construct in PBS over calvaria. Tumors were allowed to grow for five weeks and imaged the calvarial region of mice facing up towards the CCD (charge-coupled device) camera using IVIS imaging system at 20 min after luciferin (150 mg/kg, i.p). (B) Immuno-histochemical analysis of RANKL, NFATc3, p-c-Myc expression and alkaline phosphatase (ALP) activity at the tumor-bone interface in athymic mice. (C) Immunohistochemical analysis of p-c-Myc and NFATc3 expression in primary human OSCC tumor specimens and adjacent normal tissues. Data shown are representative of three replicate studies.

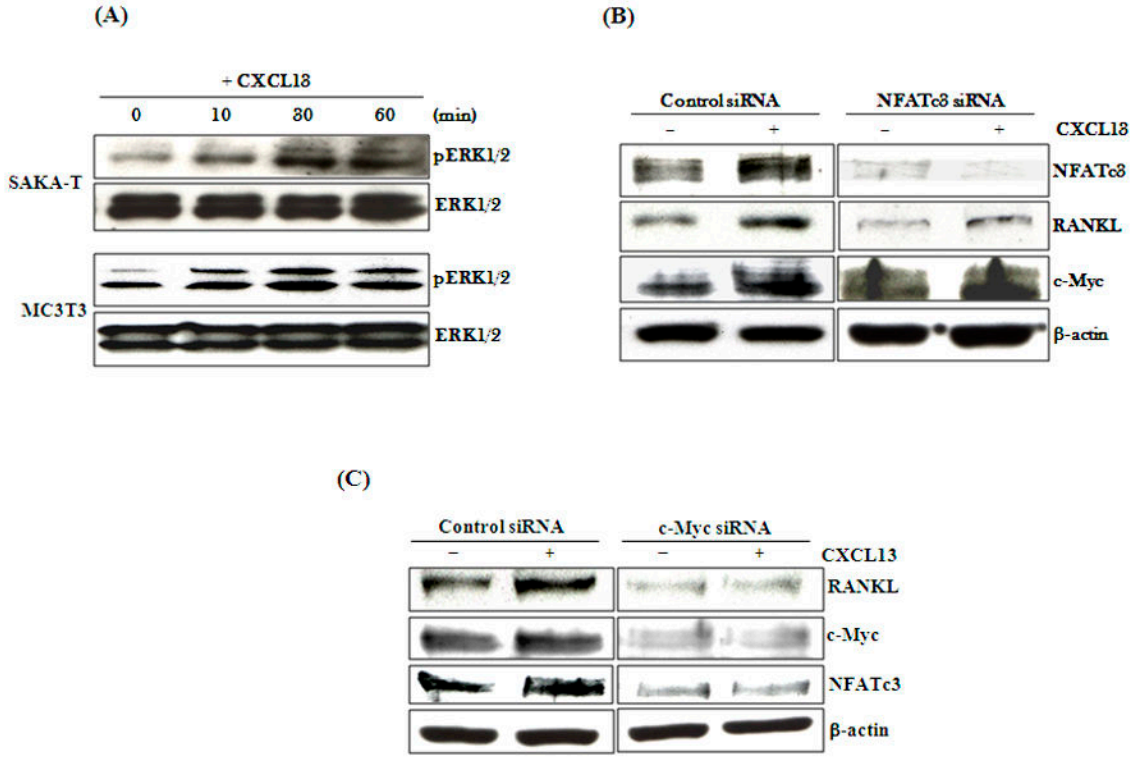

Figure 5.

CXCL13 activation of c-Myc expression induces RANKL expression. (A) CXCL13 activation of ERK1/2 in human bone marrow stromal cells (SAKA-T) and murine preosteoblast (MC3T3-E1) cells. Cells were stimulated with CXCL13 (15 ng/ml) for different time points (0–60 min) and total cell lysates were subjected to Western blot analysis for ERK1/2 and pERK1/2 expression. (B) siRNA suppression of NFATc3 inhibits RANKL but not c-Myc expression and (C) siRNA suppression of c-Myc inhibits RANKL and NFATc3 expression in MC3T3-E1 cells. Cells were transiently transfected with double stranded siRNA against c-Myc or NFATc3 using oligofectamine. After 48 h, cells were treated with CXCL13 (15 ng/ml) for 6 h and total cell lysates were analyzed by Western blot for RANKL, c-Myc and NFATc3 expression. β-actin expression serves as control. Data shown are representative of three independent experiments.

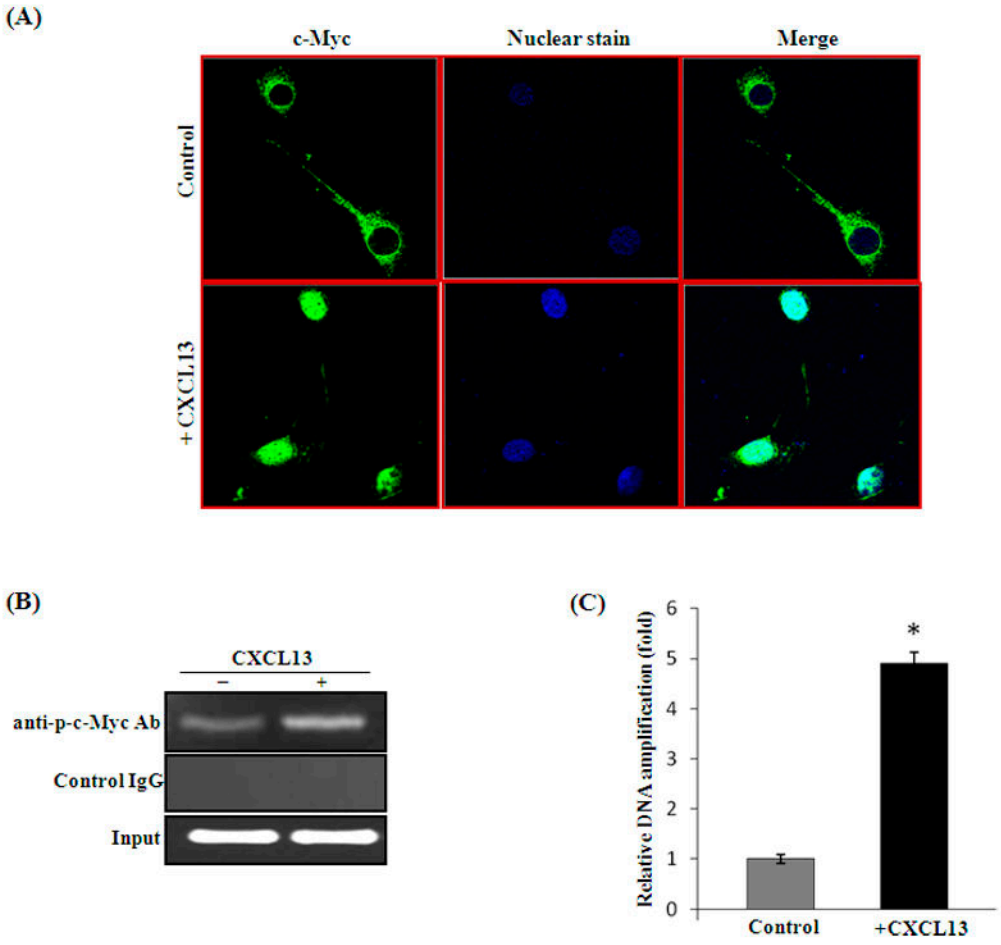

Figure 6.

CXCL13 induces c-Myc activation in human bone marrow derived stromal cells (SAKA-T) and murine preosteoblast (MC3T3-E1) cells. (A) MC3T3-E1 cells were stimulated with CXCL13 (15 ng/ml) for 6 h and c-Myc nuclear translocation was analyzed by confocal microscopy. (B) ChIP assay for c-Myc binding to hRANKL promoter region. SAKA-T cells were stimulated with and without CXCL13 (15 ng/ml) for 6 h and ChIP assay for c-Myc binding to hRANKL promoter was performed as described in methods. (C) Quantitative real-time PCR analysis of chromatin immune complexes for p-c-Myc binding to RANKL promoter region. The DNA amplification was normalized with respect to input. Data represent triplicate studies and mean ± SD (*$p<0.05$).